Article

Free Energy of Adsorption of Water and Metal Ions on the {101#4} Calcite Surface

Sebastien Kerisit, and Stephen C. Parker

J. Am. Chem. Soc., **2004**, 126 (32), 10152-10161• DOI: 10.1021/ja0487776 • Publication Date (Web): 24 July 2004

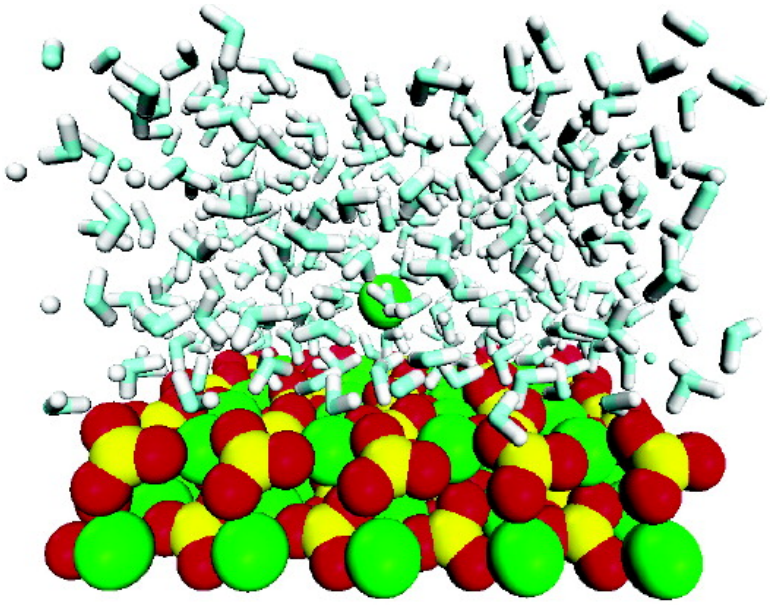

J|A|C|S
ARTICLES
Published on Web 07/24/2004

Free Energy of Adsorption of Water and Metal Ions on the {10$\bar{1}$4} Calcite Surface

Sebastien Kerisit and Stephen C. Parker*

Contribution from the Department of Chemistry, University of Bath, Claverton Down, Bath BA2 7AY, UK

Received March 3, 2004; E-mail: s.c.parker@bath.ac.uk

Abstract: We calculated the free energy profiles of water and three metal ions (magnesium, calcium, and strontium) adsorbing on the {10$\bar{1}$4} calcite surface in aqueous solution. The approach uses molecular dynamics with parametrized equations to describe the interatomic forces. The potential model is able to reproduce the interactions between water and the metal ions regardless of whether they are at the mineral surface or in bulk water. The simulations predict that the free energy of adsorption of water is relatively small compared to the enthalpy of adsorption calculated in previous papers. This suggests a large change in entropy associated with the water adsorption on the surface. We also demonstrate that the free energy profile of a metal ion adsorbing on the surface correlates with the solvent density and that the rate of formation of an innersphere complex depends on overcoming a large free energy barrier, which is mainly electrostatic in nature. Furthermore, comparison among the rates of desorption of magnesium, calcium, and strontium from the calcite surface suggests that magnesium has a much lower rate of desorption due to its strong interactions with both water and the surface.

Introduction

An important requirement for understanding and thus controlling the growth of materials at the atomic level is the ability to calculate the free energy and hence the rates of adsorption and desorption of atoms and molecules to surfaces. Many research groups have been very successful in studying the growth and dissolution of minerals using atomistic models.[1−7] However, these studies concentrate on the calculation of the energetics of different surface processes. While these calculations yield novel and interesting results, they do not contain kinetic information. In this paper, we show that atomistic techniques can evaluate the kinetic data. We consider a flat and stoichiometric surface, namely the {10$\bar{1}$4} calcite surface, in contact with an aqueous solution. The {10$\bar{1}$4} calcite surface is a good example of a simple surface, which has been studied with different computational methods,[8−10] and in each case good agreement with the available experimental data is shown. Moreover, it is by far the most dominant surface of one of the most common minerals in both geological and biological systems. Thus it has been the subject of many experimental studies.[11−16] We demonstrate the viability of the simulation methods by calculating the free energy profile of a water molecule approaching the surface and computing its residence time and diffusion coefficient at different heights above the surface. Then, we follow a similar procedure to evaluate the free energy profile of three alkaline-earth cations, magnesium, calcium, and strontium, adsorbing on the surface thereby beginning the growth process. Calculation of free energy profiles is not new; for example, free energy profiles of gases diffusing across the liquid/vapor interface,[17] ions transporting through the liquid/liquid interface,[18] and small molecules transporting through supported water films[19] have all been considered previously. However, to the best of our knowledge, this technique has not been used to investigate the adsorption of the solvent and impurity ions on a mineral surface or been used to provide kinetic information on the growth and dissolution processes. However before describing the simulation of free energies, we discuss the simulation methods.

(1) Becker, U.; Risthaus, P.; Bosbach, D.; Putnis, A. *Mol. Simul.* **2002**, *28*, 607.
(2) deLeeuw, N. H. *J. Phys. Chem. B* **2002**, *106*, 5241.
(3) Ojo, S. A.; Slater, B.; Catlow, C. R. A. *Mol. Simul.* **2002**, *28*, 591.
(4) Braybook, A. L.; Heywood, B. R.; Jackson, R. A.; Pitt, K. *J. Cryst. Growth* **2002**, *243*, 336.
(5) deLeeuw, N. H.; Harding, J. H.; Parker, S. C. *Phys. Rev. B* **1999**, *60*, 13792.
(6) Wright, K.; Cygan, R. T.; Slater, B. *Geochim. Cosmochim. Acta* **2002**, *66*, 2541.
(7) Sayle, D. C.; Parker, S. C. *J. Am. Chem. Soc.* **2003**, *125*, 8581.
(8) Kerisit, S.; Parker, S. C. *J. Phys. Chem. B* **2003**, *107*, 7676.
(9) Parker, S. C.; Kerisit, S.; Marmier, A.; Grigoleit, S.; Watson, G. W. *Faraday Discuss.* **2003**, *124*, 155.
(10) Rohl, A. L.; Wright, K.; Gale, J. D. *Am. Mineral.* **2003**, *88*, 921.
(11) Fenter, P.; Geissbuhler, P.; DiMasi, E.; Srajer, G.; Sorensen, L. B.; Sturchio, N. C. *Geochim. Cosmochim. Acta* **2000**, *64*, 1221.
(12) Paquette, J.; Reeder, R. J. *Geochim. Cosmochim. Acta* **1995**, *59*, 735.
(13) Astilleros, J. M.; Pina, C. M.; Fernandez-Diaz, L.; Putnis, A. *Geochim. Cosmochim. Acta* **2002**, *66*, 3177.
(14) Davis, K. J.; Dove, P. M.; DeYoreo, J. J. *Science* **2000**, *290*, 1134.
(15) Hoffmann, U.; Stipp, S. L. S. *Geochim. Cosmochim. Acta* **2001**, *65*, 4131.
(16) Liang, Y.; Lea, A. S.; Baer, D. R.; Engelhard, M. H. *Surf. Sci.* **1996**, *351*, 172.
(17) Somasundaram, T.; Lynden-Bell, R. M.; Patterson, C. H. *Phys. Chem. Chem. Phys.* **1999**, *1*, 143.
(18) Dang, L. X. *J. Phys. Chem. B* **1999**, *103*, 8195.
(19) Marmier, A.; Hoang, P. N. M.; Girardet, C.; Lynden-Bell, R. M. *J. Chem. Phys.* **1999**, *111*, 4862.

10.1021/ja0487776 CCC: $27.50

Table 1. Dimer and Liquid Water Properties (See Reference 27 for Definitions of θa and θd)

property	Buckingham	9–6 LJ	experiment	ab initio
		Water Dimer		
r O−O/Å	2.97	2.87	2.98[a]	2.82
θa	28.0	34.3	57.0[a]	53.9
θd	47.6	50.3	51.0[a]	56.6
$E_{binding}$ (eV)	−0.21	−0.23	−0.23[b]	−0.29
		Liquid Water		
G_{OO} (Å)	3.02 (3.80)	2.92 (3.17)	2.73 (2.83)[c]	
E_i (kJ/mol)	−52.1	−44.7	−41.7	
ρ (g.cm^{-3})	1.37	1.27	1.00	
D (10^{-9} m^2/s)	1.2	2.3	2.3	

[a] Reference 70. [b] Reference 71. [c] Reference 72.

Methods

We used atomistic simulation techniques based on the Born model of solids[20] where the solid is assumed to be comprised of ions and the interactions between atoms are separated into long-ranged electrostatic forces and short-range interactions. The short-range forces include a representation of the electron cloud repulsion, van der Waals attraction, and, where appropriate, many body terms and are modeled using parametrized functions. The latter includes an angle-dependent term reproducing covalent effects in the carbonate anion and a shell model, after Dick and Overhauser,[21] to simulate the ionic polarizability of the oxygen ions. In this model, the oxygen ion is represented as a core plus a shell coupled by a harmonic spring, and the total charge is separated between the core and the shell.

The parameters used for calcite were derived by Pavese et al.[22] in 1996 and has been used successfully by us[8,23−25] and others.[2,26] Recently, we compared the relative stability of the main low index surfaces of calcite as calculated by the Pavese potential with electronic structure calculations and found good agreement.[9] The intra- and intermolecular interactions of water were obtained from molecular dynamics simulation of liquid water.[27] We modified the hydrogen bond potential, as described in the results section, because our preferred water shell model was shown to freeze after a few hundred picoseconds[28] of molecular dynamics (MD) simulation at 300 K and zero pressure. The potential parameters for the interactions between water molecules and the calcite surface are reported in a previous paper on the water adsorption on calcite.[29] The use of molecular dynamics forced us to re-examine the model, and we have thus recently included a repulsive potential between the carbon atom in the carbonate group and the oxygen atom of the water molecules as introduced in a recent paper,[8] mainly to avoid unrealistic close contacts in molecular dynamics simulations. The magnesium and strontium interactions with water and with the calcite surface were taken from papers on metal ion segregation on calcite surfaces.[2,25] These potentials were derived from the solid-state properties; however, after testing them against electronic structure calculations, we needed to redefine the strontium− and magnesium−water potentials to remove inconsistencies. All the potential parameters used in this work are reported in Table 1 of the Supporting Information.

We performed MD simulations using the computer code DL_POLY.[30] The systems were simulated in the NVT (constant number of particles, volume, and temperature) and NPT (constant number of particles, pressure, and temperature) ensembles by use of the Nose−Hoover thermostat[31] and the Hoover barostat[31,32] with parameters for a relaxation time of 0.5 ps. The Coulombic interactions were calculated using the smooth particle mesh Ewald sum (SPME)[33] with a real space cutoff of 8 Å. The same cutoff was used for the short-range interactions. The program uses the minimum-image convention. The trajectories were generated using the Verlet Leapfrog algorithm using a time step of 0.2 fs. The shells were given a mass of 0.2 au.

These methods require reliable potential models. Thus another issue we wanted to address is the transferability of potential parameters describing the interatomic forces. Ideally, we would like to have one set of parameters to describe the interactions between water and different metal ions whether they are in bulk water or at the mineral surface or indeed in a hydrated mineral. Previous papers demonstrated that these potential parameters performed very well in reproducing ab initio calculations and experimental data of water adsorption on carbonate minerals.[9,23] Therefore, we want to investigate to what extent the same potential parameters can be used reliably to model the hydration of metal ion in solution.

Results

Water Potential. In a recent paper, van Maaren et al.[28] introduced a new shell model potential for modeling water and also compared it with various polarizable water models including the de Leeuw−Parker potential.[23] When performing a 1.3 ns long MD simulation of pure water using the de Leeuw−Parker potential, they found a phase transition after about 1 ns indicating that the system was freezing. This phase transition was not observed in the original paper because of the short length of the simulation, i.e., 150 ps. We present here a modified version of the de Leeuw−Parker potential where the hydrogen bond potential function has been replaced by a 9−6 Lennard−Jones type function. What also motivated the choice of changing the potential function is the fact that the Buckingham potential used previously was extremely attractive at short distances, which could cause unrealistic contacts between the oxygen and hydrogen atoms in MD simulations. Table 1 shows the water dimer properties obtained with the modified potential as well as the experimental and ab initio values obtained from density functional theory (DFT)(with ultrasoft Vanderbilt pseudopotentials[34,35] and generalized gradient approximation (GGA) with Perdew exchange-correlation potential[36]) using the computer code VASP[37−40] (Vienna ab initio simulation package).

We then performed an MD simulation at 300 K and zero pressure of a cubic box containing 256 water molecules in the NPT ensemble for 1.3 ns using both the original and modified water potentials. As observed by van Maaren et al.,[28] although earlier on in the simulation, we found an increase in density and a decrease in the water diffusion coefficient and intermolecular energy, revealing that the water molecules were crystallizing. The modified water potential did not show any evidence

(20) Born, M.; Huang, K. *Dynamical Theory of Crystal Lattices*; Oxford University Press: Oxford, U.K., 1954.
(21) Dick, B. G.; Overhauser, A. W. *Phys. Rev.* **1958**, *112*, 90.
(22) Pavese, A.; Catti, M.; Parker, S. C.; Wall, A. *Phys. Chem. Miner.* **1996**, *23*, 89.
(23) deLeeuw, N. H.; Parker, S. C. *J. Phys. Chem. B* **1998**, *102*, 2914.
(24) deLeeuw, N. H.; Parker, S. C. *Phys. Chem. Chem. Phys.* **2001**, *3*, 3217.
(25) deLeeuw, N. H.; Parker, S. C. *J. Chem. Phys.* **2000**, *112*, 4326.
(26) Duffy, D. M.; Harding, J. H. *J. Mater. Chem.* **2002**, *12*, 3419.
(27) deLeeuw, N. H.; Parker, S. C. *Phys. Rev. B* **1998**, *58*, 13901.
(28) vanMaaren, P. J.; vanderSpoel, D. *J. Phys. Chem. B* **2001**, *105*, 2618.
(29) deLeeuw, N. H.; Parker, S. C. *J. Chem. Soc., Faraday Trans.* **1997**, *93*, 467.
(30) DL_POLY is a package of molecular simulation routines written by W. Smith and T. R. Forester, copyright The Council for the Central Laboratory of the Research Councils, Daresbury Laboratory at Daresbury, Nr. Warrington, 1996.
(31) Hoover, W. G. *Phys. Rev. A* **1985**, *31*, 1695.
(32) Melchionna, S.; Ciccotti, G.; Holian, B. L. *Mol. Phys.* **1993**, *78*, 533.
(33) Essmann, U.; Perera, L.; Berkowitz, M. L.; Darden, T.; Lee, H.; Pedersen, L. G. *J. Chem. Phys.* **1995**, *103*, 8577.
(34) Vanderbilt, D. *Phys. Rev. B* **1990**, *41*, 7892.
(35) Kresse, G.; Hafner, J. *J. Phys.: Condens. Matter* **1994**, *6*, 8245.
(36) Perdew, J. P.; Chevary, J. A.; Vosko, S. H.; Jackson, K. A.; Pederson, M. R.; Singh, D. J.; Fiolhais, C. *Phys. Rev. B* **1992**, *46*, 6671.
(37) Kresse, G.; Hafner, J. *Phys. Rev. B* **1993**, *47*, 558.
(38) Kresse, G.; Furthmuller, J. *Phys. Rev. B* **1996**, *54*, 11169.
(39) Kresse, G.; Furthmuller, J. *Comput. Mater. Sci.* **1996**, *6*, 15.
(40) Kresse, G.; Hafner, J. *Phys. Rev. B* **1994**, *49*, 14251.

of freezing in the time scale of the simulation (see Supporting Information S1). Moreover, the most significant properties, such as the average intermolecular energy, density, and diffusion coefficient, were improved relative to the experimental values as shown in Table 1. Furthermore, its key asset remains; namely, it is compatible with the potential models used for solid oxides and minerals, and thus we can be confident that our water−mineral interface is reliable over long simulation time scales.

Interaction of Metal Ions with Water. A further requirement of modeling the solid−water interface is that we need a robust way of testing the reliability of the interactions of isolated ions such as calcium, magnesium, and strontium with water. The potential model parameters, initially derived from the solid state, are tested by comparing first with DFT calculations of gas phase clusters to evaluate the energetics, then with experimental data of ions in solution to provide structural information, and finally with rate data to give a test of the free energy.

A. Cation−Water Gas-Phase Clusters. We used the computer code DL_POLY[30] to perform 0 K calculations with direct Coulombic summation and no periodic boundary conditions to model $[Ca(H_2O)_n]^{2+}$, $[Mg(H_2O)_n]^{2+}$, and $[Sr(H_2O)_n]^{2+}$ clusters where $n = 1-9$. All $[Ca(H_2O)_9]^{2+}$ and $[Sr(H_2O)_9]^{2+}$ clusters relaxed to a complex with eight molecules in the first hydration shell and one in the second shell. All magnesium−water complexes with $n > 6$ relaxed to have only six water molecules in their first shell. The energetically preferred configuration of the $[Ca(H_2O)_8]^{2+}$ and $[Sr(H_2O)_8]^{2+}$ complexes is the square antiprism, whereas the $[Mg(H_2O)_6]^{2+}$ complex is octahedral. The results were then compared with recent gas-phase cluster computational studies that use a high level of calculation. Calcium−water cluster calculations by Bako et al.,[41] who used localized basis set (6-311+G**) DFT at the BLYP level found, as we did, that a ninth water molecule cannot be added to the first calcium hydration shell. They obtained calcium−oxygen distances, ranging from 2.248 Å for $n = 1$ to 2.510 Å for $n = 8$ and hydrogen−oxygen distances from 0.986 to 0.972 Å. This compares well with our calcium−oxygen and hydrogen−oxygen distances, which range from 2.26 to 2.51 Å and 0.983 to 0.978 Å, respectively. We also found the work of Pavlov et al.,[42] who used DFT B3LYP with very large basis sets to calculate the structure and energy of $[Mg(H_2O)_n]^{2+}$ complexes with $n = 1-6$. They obtained magnesium−oxygen distances going from 1.94 Å for $n = 1$ to 2.08 Å for $n = 6$. Again, the cation−oxygen distances agree well with our calculations: from 1.95 for $n = 1$ to 2.07 Å for $n = 6$. Table 2 compares the hydration energies calculated by Bako et al.[41] and Pavlov et al.[42] with those obtained in this work. The binding energies, E_{TOT}, and the energy to remove a water molecule from a cluster, ΔE, were obtained according to

$$E_{TOT} = (E_{[X(H_2O)_n]^{2+}} - nE_{H_2O})/n \quad (1)$$

$$\Delta E = E_{[X(H_2O)_n]^{2+}} - E_{H_2O} - E_{[X(H_2O)_{n-1}]^{2+}} \quad (2)$$

Table 2 shows that the binding energies are systematically underestimated because of the lack of electronic relaxation of the potential model. However, the agreement between the two types of calculations improves as the number of water molecules increases. Also, the trends in E_{TOT} and ΔE are reproduced. One interesting point to note from Table 2 is that adding a molecule to the second cation shell is energetically favored for calcium but not for magnesium. In both cases two molecules from the first shell form a hydrogen bond with the new molecule. However, with calcium, due to the shape of the cluster, there is less relaxation than with magnesium and the hydrogen bonds are shorter. Moreover, we expect the calcium−water potential to be much broader than the magnesium−water potential, which implies a smaller energy penalty for deviations from the optimum geometry. To the best of our knowledge, there is no ab initio calculation of strontium−water clusters in the gas phase. Our calculations predict hydration energies similar to those obtained for calcium (see Table 2) and strontium−oxygen distances varying from 2.45 Å for $n = 1$ to 2.62 Å when $n = 8$. In conclusion, the ion−oxygen distances and the water geometry for both calcium− and magnesium−water complexes agree with electronic structure calculations for different cluster sizes. Also, our atomistic potentials reproduce energy differences between clusters when the number of water molecules is high. This is reassuring as ultimately we are interested in studying those cations in solution.

Table 2. Calculated Energetics for a Cluster Containing M^{2+} with *n* Water Molecules (M = Ca, Sr, or Mg)

n	E_{TOT} (eV) this work	E_{TOT} (eV) DFT[41,42]	ΔE (eV) this work	ΔE (eV) DFT[41,42]	E_{TOT} (eV) this work	ΔE (eV) this work
		Calcium				Strontium
1	−1.586	−2.476	−1.586	−2.476	−1.354	−1.354
2	−1.560	−2.277	−1.533	−2.078	−1.334	−1.313
3	−1.521	−2.169	−1.442	−1.952	−1.303	−1.242
4	−1.479	−2.028	−1.353	−1.566	−1.270	−1.172
5	−1.423	−1.865	−1.203	−1.145	−1.231	−1.074
6	−1.378	−1.734	−1.149	−1.070	−1.196	−1.024
7	−1.290	−1.573	−0.760	−0.571	−1.141	−0.810
8	−1.222	−1.452	−0.748	−0.561	−1.095	−0.769
8 + 1	−1.262		−1.586		−1.111	−1.238
			Magnesium			
1	−2.422	−3.534	−2.422	−3.534		
2	−2.379	−3.304	−2.336	−3.074		
3	−2.310	−2.999	−2.173	−2.389		
4	−2.229	−2.725	−1.985	−1.904		
5	−2.068	−2.421	−1.424	−1.214		
6	−1.961	−2.196	−1.429	−1.062		
6 + 1	−1.800		−0.831			
6 + 2	−1.664		−0.714			
6 + 3	−1.597		−1.057			

B. Cation Hydration in Solution. We then used DL_POLY to perform 1 ns simulations of a cation, in a cubic box, with 255 water molecules. The simulations were performed at 300 K and zero pressure in the NPT ensemble. The first peak of the radial distribution functions (RDF) is located at 2.08, 2.43, and 2.63 Å for magnesium, calcium, and strontium, respectively. Their respective first hydration shells extend to 2.5, 3.5, and 3.6 Å with average coordination numbers of 6, 8.2, and 8.9. Ohtaki and Radnai[43] reported, in their review on hydration of ions, average magnesium−oxygen distances from X-ray diffraction studies between 2.00 and 2.15 Å and coordination numbers of 6 for most studies, in agreement with our results. A recent ab inito MD calculation of a magnesium ion in water by Lightstone et al.[44] showed similar results too, namely a

(41) Bako, I.; Hutter, J.; Palinkas, G. *J. Chem. Phys.* **2002**, *117*, 9838.
(42) Pavlov, M.; Siegbahn, P. E. M.; Sandstrom, M. *J. Phys. Chem. A* **1998**, *102*, 219.
(43) Ohtaki, H.; Radnai, T. *Chem. Rev.* **1993**, *93*, 1157.
(44) Lightstone, F. C.; Schwegler, E.; Hood, R. Q.; Gygi, F.; Galli, G. *Chem. Phys. Lett.* **2001**, *343*, 549.

magnesium−oxygen distance of 2.13 Å and a coordination number of 6. Jalilehvand et al.[45] found, using extended X-ray absorption fine structure spectroscopy (EXAFS), large-angle X-ray scattering (LAXS), and MD simulation, an average calcium−water distance of 2.46 Å with a coordination number of 8, which again agrees well with our calculations. However, while the coordination number of magnesium is almost invariably 6, calcium coordination number has been found to range from 6 to 10.[41,46−48] X-ray diffraction studies of Albright[49] and Caminiti et al.[50] showed strontium−oxygen distances of 2.60 and 2.64 Å and coordination number of 7.9 and 8, respectively. Again, the ion-oxygen distance matches our simulation but our coordination number is relatively high. However, a more recent X-ray diffraction study of strontium hydration[51] revealed a first strontium−oxygen peak at 2.67 Å with a coordination number of 8 to 9. In conclusion, our interatomic potentials, derived originally for the solid state, reproduce the structure of the first hydration shell of the three cations as found by X-ray diffraction studies and ab initio MD calculations.

C. Water Residence Time in the First Hydration Shell. To investigate the dynamics of cation hydration and to provide a comparison with the dynamics at the mineral interface, we calculated the water residence time in the first hydration shell. For calcium and strontium, this can be obtained by analysis of the direct simulation trajectories, since the water exchange rate is much faster than the length of the simulation. However, as the water exchange rate for magnesium is several orders of magnitude lower, the water residence time could only be calculated using transition state theory. First, for calcium and strontium, we calculated the water residence time from the residence-time correlation function, which is defined as[52]

$$\langle R(t)\rangle = \left\langle \frac{1}{N_0}\sum_{i=1}^{N_t}\theta_i(0)\theta_i(t)\right\rangle \tag{3}$$

where N is the number of water molecules in the first hydration shell and θ_i is the Heaviside function, which is 1 if the ith water molecule is in the first hydration shell at time t and 0 otherwise. As introduced by Impey et al.,[52] a water molecule was counted as having left the first shell if it has done so for a least 2 ps. This is to allow for water molecules which temporarily leave the first shell and come back without entering the bulk for a significant amount of time to be counted in the residence time. The residence time can then be obtained by integration of $\langle R(t)\rangle$:

$$\tau = \int_0^\infty \langle R(t)\rangle \, \mathrm{d}t \tag{4}$$

The uncertainty on the residence time was estimated as the 95% confidence interval of the mean when the trajectories were separated into six independent blocks. We obtained a residence time of 39 ± 6 ps and 38 ± 4 ps for water in the first hydration shell of calcium and strontium, respectively. Our calculation for calcium differs from that of Koneshan et al.[53] who used atomistic MD and found an average residence time of about 700 ps. However, a quasi-elastic neutron scattering (QENS) study reported an ion−water proton binding time of less than 100 ps. Also Schwenk et al.[54] who used QM/MM-MD at the Hartree−Fock (HF) and DFT level and Naor et al.[55] who used CPMD with the BLYP functional found that the water residence time in the first hydration shell was of the order of 10 ps. For strontium, our prediction agrees reasonably well with the calculations of Obst and Bradaczek,[56] who used the CHARM22 force field and found a water residence time of 50.7 ps. Moreover, Harris et al.[57] predicted, from their short DFT MD simulation, a residence time of the order of 10 ps in agreement with our calculation.

Second, we calculated the water residence time for each cation from transition state theory, where we define the reaction coordinate as the distance between the cation and the center of mass of the water molecule. The dissociation constant can be written as[58,59]

$$k = \kappa k^{\mathrm{TST}} \tag{5}$$

where k^{TST} is the transition state rate constant,[60]

$$k^{\mathrm{TST}} = \sqrt{\frac{k_{\mathrm{B}}T}{2\pi\mu}}\frac{e^{-\beta W(r^*)}}{\int_0^{r^*} e^{-\beta W(r)}\,\mathrm{d}r} \tag{6}$$

where μ is the ion−water reduced mass, β is $1/k_{\mathrm{B}}T$, and r^* is the transition state distance.

The transmission coefficient κ is determined from the plateau value of the normalized reactive flux, which can be computed as[58]

$$k(t) = \frac{\langle \dot{r}(0)\theta[r(t) - r^*]\rangle_{\mathrm{c}}}{\langle \dot{r}(0)\theta[\dot{r}(0)]\rangle_{\mathrm{c}}} \tag{7}$$

where $\theta[x]$ is the Heaviside function, which is 1 if x is larger than 0 and 0 otherwise, and $\dot{r}(0)$ is the initial ion−water velocity along the reaction coordinate. The subscript c means that the initial configurations have been generated in the constrained reaction coordinate ensemble.

The transition state rate constant requires the calculation of the free energy profile of a water molecule leaving the first hydration shell, i.e., the potential of mean force (PMF). The PMF can be calculated directly from the RDF using the following equation if the region of exchange is well sampled; that is, if the exchange rate is fast compared to the total simulation time.[61]

(45) Jalilehvand, F.; Spangberg, D.; Lindqvist-Reis, P.; Hermansson, K.; Persson, I.; Sandstrom, M. *J. Am. Chem. Soc.* **2001**, *123*, 431.
(46) Probst, M. M.; Radnai, T.; Heinzinger, K.; Bobb, P.; Rode, B. M. *J. Phys. Chem.* **1985**, *89*, 753.
(47) Hewish, N. A.; Nelson, G. N.; Howe, R. A. *Nature (London)* **1982**, *297*, 138.
(48) Palinkas, G.; Heinzinger, K. *Chem. Phys. Lett.* **1986**, *126*, 251.
(49) Albright, J. N. *J. Chem. Phys.* **1972**, *56*, 3783.
(50) Caminiti, R.; Musinu, A.; Paschina, G.; Pinna, G. *J. Appl. Crystallogr.* **1982**, *15*, 482.
(51) Ramos, S.; Neilson, G. W.; Barnes, A. C.; Capitan, M. J. *J. Chem. Phys.* **2003**, *118*, 5542.
(52) Impey, R. W.; Madden, P. A.; McDonald, I. R. *J. Phys. Chem.* **1983**, *87*, 5071.
(53) Koneshan, S.; Rasaiah, J. C.; Lynden-Bell, R. M.; Lee, S. H. *J. Phys. Chem. B* **1998**, *102*, 4193.
(54) Schwenk, C. F.; Loeffler, H. H.; Rode, B. M. *Chem. Phys. Lett.* **2001**, *349*, 99.
(55) Naor, M. N.; Nostrand: K. V.; Dellago, C. *Chem. Phys. Lett.* **2003**, *369*, 159.
(56) Obst, S.; Bradaczek, H. *J. Phys. Chem.* **1996**, *100*, 15677.
(57) Harris, D. J.; Brodholt, J. P.; Sherman, D. M. *J. Phys. Chem. B* **2003**, *107*, 9056.
(58) Chandler, D. *J. Chem. Phys.* **1978**, *68*, 2959.
(59) Yamamoto, T. *J. Chem. Phys.* **1960**, *33*, 281.
(60) Ciccotti, G.; Ferrario, M.; Hynes, J. T.; Kapral, R. *J. Chem. Phys.* **1990**, *93*, 7137.
(61) Hill, T. L. *Statistical Mechanics*; McGraw-Hill: New York, 1956.

$$W(r) = -k_B T^* \ln(g(r)) \quad (8)$$

We calculated the PMF for the calcium and strontium simulations using eq 8, but it was not possible to do so for magnesium as no exchange took place at all during the whole simulation run. Therefore, we performed a series of simulations where the distance between the magnesium ion and a water molecule is constrained at different positions from the first to the second hydration shell, i.e., from 1.8 to 3.7 Å every 0.1 Å. Figure 1 shows the PMF against the ion−water separation for the three cations. The transition state is located at 2.9, 3.5, and 3.6 Å for magnesium, calcium, and strontium, respectively. The barrier height for a water molecule to escape from the first shell is ~4 k_BT for calcium and strontium and 15k_BT for magnesium.

To compute the transmission coefficient, we first generated a pool of starting configurations by running a series of MD simulations where the separation of the cation to a selected water molecule is constrained to be the transition state distance. We recorded a configuration every 3 ps after a short equilibration period to obtain 1000 configurations. Then, each configuration is run both backward and forward in time for a short period of time, i.e., 1.4 ps. The three reactive fluxes obtained from eq 7 are presented in the Supporting Information. The resulting transmission coefficient is 0.02, 0.14, and 0.18 ± 0.02 for magnesium, calcium, and strontium, respectively. The uncertainty in the transmission coefficient is obtained by calculating the 95% confidence interval of the mean when the trajectories are separated in 12 independent blocks. We obtained a residence time of 38 ± 4 and 32 ± 7 ps for water in the first hydration shell of calcium and strontium, which agrees with the 39 ± 6 and 38 ± 4 ps obtained from the direct simulation. The fact that the transition state theory and the analysis of the direct simulation yield the same residence times for calcium and strontium within the uncertainty range gives us confidence in the methods employed in this work. The transmission coefficient for magnesium is much smaller than that of calcium and strontium and gives a water residence of 2.8 ± 1.2 μs (i.e., an exchange rate of 3.5 ± 2.6 × 10^5 s^{-1}) which agrees well with two ^{17}O NMR studies by Bleuzen et al.[62] and Neely and Connick[63] who reported a water exchange rate of 6.7 ± 0.2 10^5 s^{-1} and 5.3 ± 0.3 10^5 s^{-1}, respectively. To conclude, we have shown that potential parameters derived for the interaction of solids with water are able to reproduce the energetics, structure, and dynamics of the hydration shell of the three cations studied here. Our calculations also suggest that the residence times of water in the hydration shell of calcium and strontium are similar, whereas it is several orders of magnitude longer for magnesium. As we shall demonstrate later on in this paper, this difference has an effect on the adsorption behavior of the cations.

Free Energy of Adsorption of Water. Before considering the adsorption of metal ions on the calcite surface, we investigated the interaction of the solvent, namely water, with this surface.

A. Free Energy and Density Profiles. We performed a 1 ns MD simulation of a calcite slab in contact with bulk water, with an initial equilibration period of 40 ps. The simulation was run in the NVT ensemble at 300 K and zero pressure. The slab is about 15 Å thick with a surface area of 24.12 × 23.98 $Å^2$ and contains 180 $CaCO_3$ units. The water slab is about 20 Å thick and contains 360 water molecules, which corresponds to the optimized density for this water potential at 300 K and zero pressure, i.e., 1.3 $g.cm^{-3}$. We calculated the free energy difference between a water molecule at a height z and a water molecule in the bulk, i.e., at height z_0, by integrating the average force in the direction perpendicular to the surface, f_z, acting on the whole water molecule from z_0 to z:

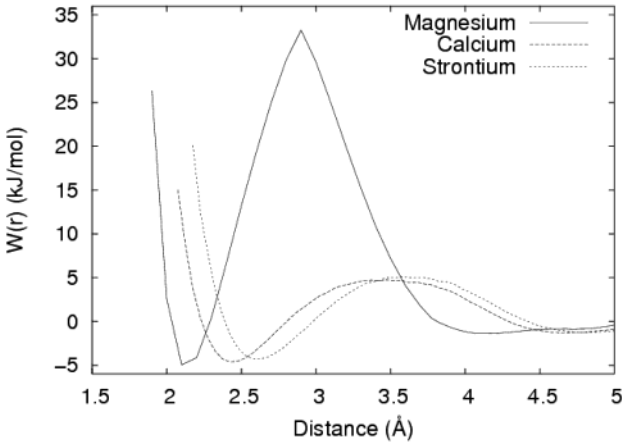

Figure 1. Calcium−, strontium−, and magnesium−water potential of mean force in bulk water.

$$\Delta A(z) = A(z) - A(z_0) = \int_{z_0}^{z} \langle f_z(z) \rangle dz \quad (9)$$

The force acting on a whole water molecule was obtained by calculating the force acting on its center of mass from the weighted force on its constituent atoms. Figure 2 shows the free energy profile of a water molecule approaching the surface as well as the water density relative to the bulk water density obtained according to

$$\rho(z) = \frac{\langle n(z) \rangle}{\langle n(z_0) \rangle} \quad (10)$$

where $n(z)$ is the number of water molecules with their center of mass at a height z. Figure 2 shows a clear layering of the water in the vicinity of the surface, which has been seen before, in both theoretical[64] and experimental studies.[65] As one would expect, the two profiles have a "mirror symmetry", where zones of high density coincide with free energy wells. The first two density peaks suggest the presence of two water molecules in the hydration layer at an average height of 2.2 and 3.2 Å. Our results are in very good agreement with the heights obtained from recent X-ray scattering data:[66] 2.3 ± 0.1 and 3.5 ± 0.2 Å. We will refer to these two modes of adsorption as mode I and II, respectively. The first two peaks are followed by a wide region of very low water density before a third peak at 5.0 Å. Then, the amplitude of the oscillations decreases, and the density converges to almost that of bulk water (i.e., 83%) in the middle of the water slab. Visualization of the trajectories reveals that

(62) Bleuzen, A.; Pittet, P.; Helm, L.; Merbach, A. E. *Magn. Reson. Chem.* **1997**, *35*, 765.
(63) Neely, J.; Connick, R. *J. Am. Chem. Soc.* **1970**, *92*, 3476.
(64) McCarthy, M. I.; Schenter, G. K.; Scamehorn, C. A.; Nicholas, J. B. *J. Phys. Chem.* **1996**, *100*, 16989.
(65) Cheng, L.; Fenter, P.; Nagy, K. L.; Schlegel, M. L.; Sturchio, N. C. *Phys. Rev. Lett.* **2001**, *87*.
(66) Fenter, P. Private communications.

mode I corresponds to water molecules bonded to a surface calcium via their oxygen atom and mode II corresponds to those that form a hydrogen bond with a surface oxygen. Both modes have very similar free energies of adsorption, i.e., −2.8 and −2.4 kJ/mol for mode I and II, respectively. Therefore, it is not surprising that the two modes of adsorption have an almost 1:1 ratio. Indeed, the average coordination per surface calcium is 1.01 (mode I) and 0.86 per surface oxygen (mode II). The free energies of adsorption calculated here are surprisingly low compared to the enthalpy of adsorption reported in previous papers (about −45 kJ/mol).[8,23] This, therefore, implies a large entropy change associated with the adsorption of water molecules on the surface, which almost compensates the enthalpy term.

B. Water Structure and Dynamics near the Interface. As a way of understanding the bonding mechanism with the surface, we calculated the orientation order parameter as function of distance to the surface. The orientation order parameter is given by[67]

$$S\phi(z) = \left\langle \frac{1}{N_z}\sum_{i=1}^{N_z}\frac{1}{2}(3\cos^2\theta_i - 1)\right\rangle \qquad (11)$$

where θ_i is the angle between the water dipole moment and the normal to the surface and N_z is the number of water molecules at a distance z from the surface. A value of −0.5 means that the water dipole is at right angles to the normal of the surface, and a value of 1 indicates that it is perpendicular to the surface. Figure 2 shows the clear ordering of the water orientation in the first few angstroms of the surface compared to that in the bulk. In the first layer, the water molecules that get closer than 2 Å flatten out. Furthermore, $S\phi$ increases from −0.4 to about 0.3 and then sharply decreases to almost zero at the boundary with the second layer. This probably indicates that the water molecules rotate as they move away from the surface to form hydrogen bonds with other water molecules and then quickly reorientate upon entrance in the second layer. We can also see a similar sharp change in orientation at the limit between the second and third layer. In the third layer, the water molecules still show some order in their orientation, and further away from the surface, the water orientation does not seem to be completely random. The effect of the calcite surface on the water diffusion is investigated by calculating the diffusion coefficient in the directions perpendicular and parallel to the surface as a function of distance from the mean-square displacement (MSD) of the water molecules. We considered the z coordinate to obtain the MSD in the direction perpendicular to the surface:[68]

$$D(z) = \lim_{t\to\infty}\langle (z(t) - z(0))^2\rangle/2t \qquad (12)$$

And similarly, we considered the x and y coordinate to plot the diffusion in the direction parallel to the surface. As water molecules explore regions with different diffusion coefficients within the time scale of our simulation, we only considered short time trajectories, i.e., 5 ps, as introduced by Marrink and Berendsen.[68] The geometric center of the 5 ps trajectory determined the position along the normal to the surface. The diffusion profiles are plotted in Figure 2 together with the water

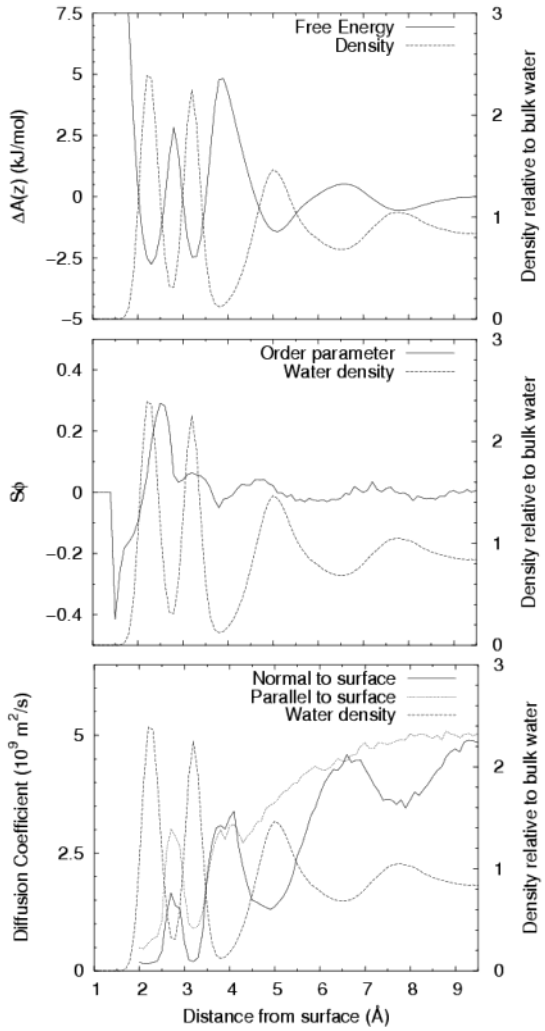

Figure 2. Water density, free energy profile, orientation order parameter, and self-diffusion coefficient as a function of distance from the surface.

density. There are several points to take from this figure. First, it is clear that the diffusion coefficient decreases in both directions as the molecules approach the surface. Second, the diffusion is isotropic in the bulk region but is anisotropic almost everywhere else. The diffusion in the direction normal to the surface is well correlated with the water layering; i.e., water has a high diffusion coefficient in a region of low density, whereas the diffusion parallel to the surface smoothly decreases up to the second layer and only starts to show some correlation with the water density from about 4 Å. In the first two layers, the water diffusion is greatly reduced with a diffusion coefficient of 0.2 10^{-9} m^2/s or less in the direction normal to the surface and about 0.6 10^{-9} m^2/s in the first layer and 0.9 10^{-9} m^2/s in the second layer in the direction parallel to the surface. Also, we calculated the diffusion coefficient in the middle of the water slab to be about twice that in bulk water; this is probably due, as pointed out earlier, than the water density in that region is 83% that of bulk water. To determine whether the reduced density in the middle of the slab affects the water structure to a large extent, we calculated the oxygen−oxygen RDF of water in each layer as shown in the Supporting Information. We found that the water structure in the middle of the slab (layer 4) is not significantly different from that of bulk water. Although we expect the change in the free energy of adsorption to be at a

(67) Stockelmann, E.; Hentschke, R. *J. Chem. Phys.* **1999**, *110*, 12097.
(68) Marrink, S. J.; Berendsen, J. C. *J. Phys. Chem.* **1994**, *98*, 4155.

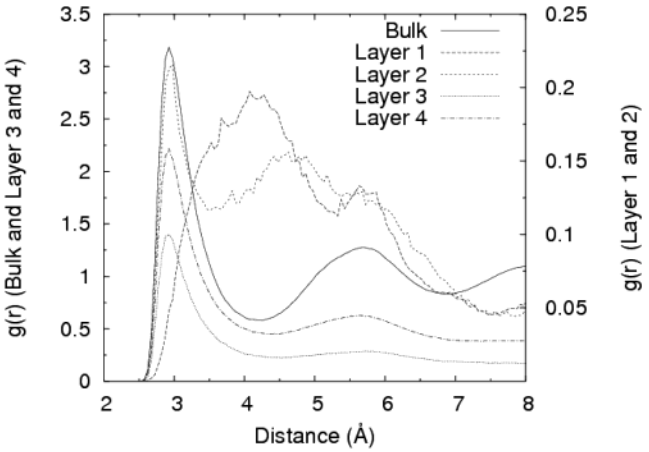

Figure 3. Intralayer oxygen−oxygen RDF.

Table 3. Water Residence Time in the Different Water Layers above the Calcite Surface

water layer	layer thickness (Å)	residence time (ps)
1	1.3	300 ± 17
2	1.0	53 ± 5
3	2.7	16 ± 1
4	3.0	8.8 ± 0.5

minimum, it would be worth simulating the same system with a much thicker water slab, when our computer resources allow us. We also calculated the intralayer oxygen−oxygen RDF (Figure 3). The first hydration layer does not show a peak at 2.92 Å but instead shows a very broad peak centered at about 4.1 Å, which corresponds to the shortest calcium−calcium distance at the surface. Therefore, we can conclude that the hydrogen bond network within the first layer is completely disrupted. The second hydration layer shows a peak at 2.92 Å as well as a broad peak centered at about 4.9 Å, which coincides with a carbonate oxygen−carbonate oxygen distance at the surface. Hence the interaction with the surface is not strong enough in this layer to break completely the water hydrogen bond network. The water diffusion was further investigated by computing the residence time of water molecules in the different layers above the surface using eqs 3 and 4. Table 3 demonstrates that the residence time of a water molecule increases considerably as it approaches the surface. It also shows that the residence time in the first layer is 1 order of magnitude longer than that in the first hydration shell of an isolated calcium ion. The analysis of the water orientation order parameter, diffusion coefficient, and residence time strongly suggests that the rotational and translational degrees of freedom are reduced to a great extent upon adsorption on the calcite surface, which supports our suggestion of a large entropy change postulated earlier on.

Free Energy of Adsorption of Metal Ions. A. Free Energy Profiles. The free energy profiles of magnesium, strontium, and calcium ions as a function of distance to the surface were obtained by running a series of MD simulations where the metal ion is constrained at different heights above the surface. Fifty calculations were performed to obtain points between $z = 2.5$ Å and $z = 10$ Å. In each calculation, a water molecule is replaced by the metal ion and the system is equilibrated for 10 ps in the NVT ensemble. Then, the force in the direction normal to the surface is averaged over a further 150 ps. Figure 4 shows

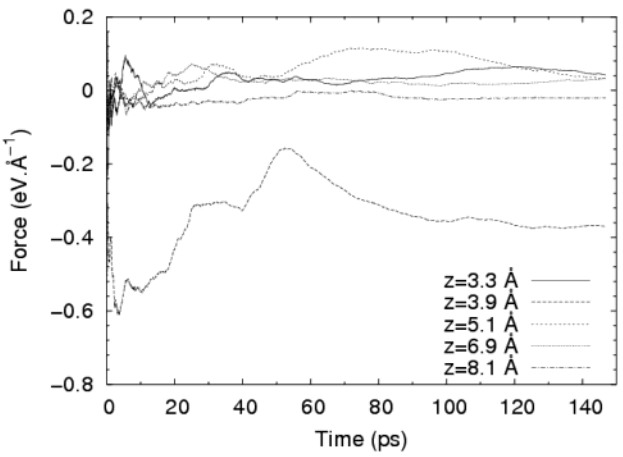

Figure 4. Running average force in the direction normal to the surface on a fixed calcium ion at different heights above the surface.

the running average of the force as a function of time for calcium at five different heights above the surface. While they all seem to be converged within the time scale of the simulation, the force on the calcium ion when it is positioned at the top of the free energy barrier shows large fluctuations. The free energy profiles are obtained according to eq 9 and shown in Figure 5 together with the water density. The error bars were estimated by calculating the 95% confidence interval of the mean when dividing the simulation into six blocks. All figures show that the relative free energy as a function of distance from the surface is correlated with the water density with the largest free energy barrier coinciding with the region of lowest water density. There are two main energy wells at about 3 and 5 Å, which correspond to the formation of the inner- and outersphere complexes. The metal ions adsorb as an innersphere complex directly above a surface carbonate group at a height of 3.2, 3.3, and 3.4 Å for magnesium, calcium, and strontium, respectively. As shown in Figure 6 at this height, the metal ions are all coordinated to one carbonate oxygen from the surface and their first coordination shell is completed with the oxygen atoms of water: the water coordination of these ions are 5.0 for magnesium, 6.6 for calcium, and 7.3 for strontium. In addition, at this height, the average cation−water oxygen distance is 2.08, 2.42, and 2.62 Å for magnesium, calcium, and strontium respectively, i.e., exactly the same distances as those found in bulk water. Thus both calcium and strontium, when close to the surface, have partially incomplete first coordination shells compared to their coordination in bulk water, whereas magnesium retains its overall coordination of 6. The cation−carbonate oxygen distance is 1.98, 2.27, and 2.42 Å for magnesium, calcium, and strontium, respectively. MD simulations of the respective pure cation carbonate at the same temperature and pressure give average cation−carbonate oxygen distances of 2.08, 2.32, and 2.52 Å. Indeed, the preferred site corresponds to a cation lattice site if the crystal was extended, but the presence of the surface and its effect on the water structure prevent the calcium and strontium ions from having a complete coordination shell. We suggest that there is a competition for water molecules between the surface and the adsorbed ion. The residence time of water molecules at the surface and in the first hydration shell of the metal ions is directly related to the strength of the bond with water. In the cases of calcium and strontium, the strength of the water−cation bond is similar, although slightly weaker, to

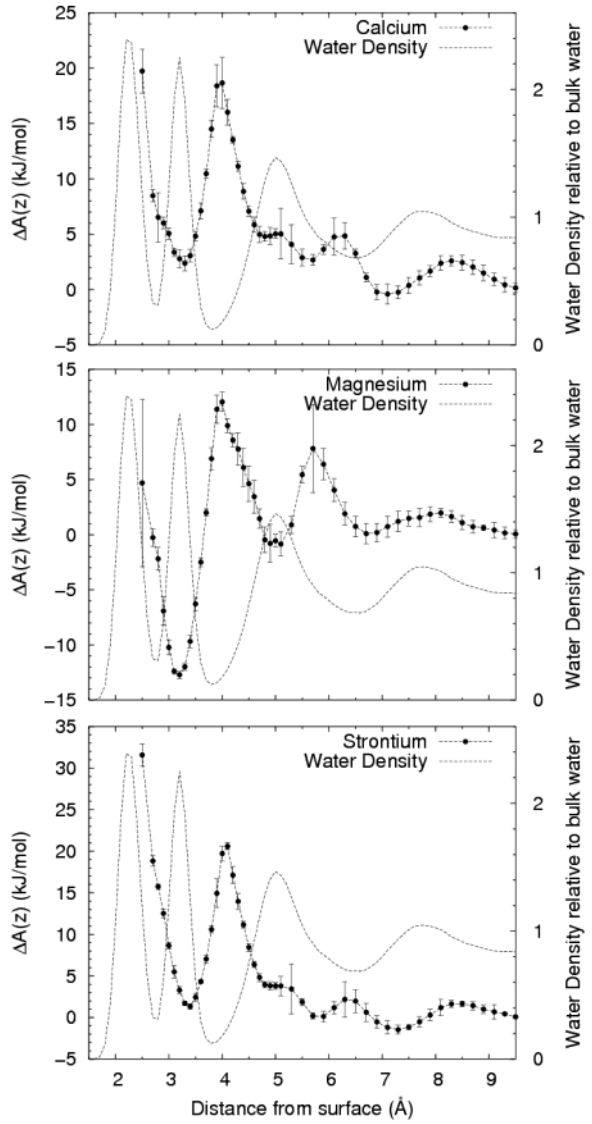

Figure 5. Calcium, magnesium, and strontium free energy profile as a function of distance from the surface.

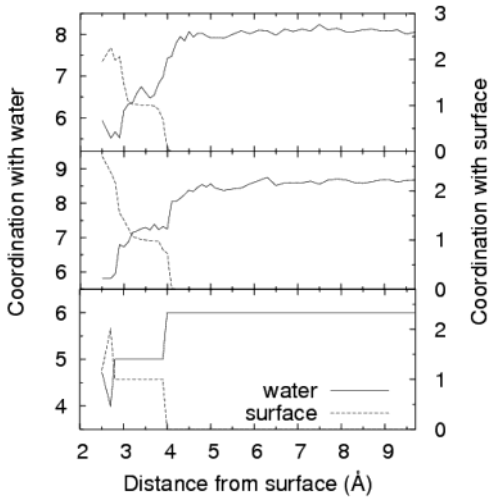

Figure 6. Metal ion coordination with water and the surface as a function of distance from the surface: (top) calcium, (middle) strontium, (bottom) magnesium.

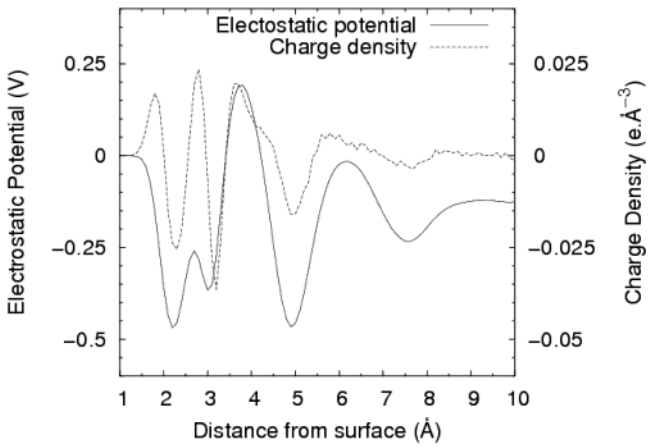

Figure 7. Charge density and electrostatic potential as a function of distance from the surface.

that of the water−surface bond. Magnesium however forms a much stronger bond with water and is therefore able to attract water molecules from the surface to retain a full coordination shell. Moreover magnesium has a lower coordination, which is also the same as the cation coordination in the calcite structure. Hence, the strong magnesium−surface interaction and the fact that magnesium can disrupt the surface hydration layers greatly favor the formation of an innersphere complex over the outersphere complex by about 10 kJ/mol, whereas for calcium and strontium the innersphere complex is lower in free energy than the outersphere complex by about 2 kJ/mol. The outersphere complexes are positioned, for all cations, at 4.9 Å above the surface. As seen with the innersphere complexes, the average cation−water oxygen distance is not affected by the presence of the surface; however, the average coordination number of calcium and strontium decreases slightly to 8.0 and 8.5, respectively, whereas that of magnesium remains 6.0. The position of the transition state between the inner- and outersphere complexes is almost identical for the three cations, i.e., at about 4.0 Å. Figure 6 reveals that this position coincides with the exchange, in the cation first coordination shell, of a water molecule with an oxygen atom from the surface. Hence the distance at which this exchange occurs does not seem to be dependent on the size of the ion. The height of the free energy barrier of adsorption is also very similar for all three cations: 12.8, 13.9, and 16.8 kJ/mol for magnesium, calcium, and strontium, respectively.

B. Origin of the Free Energy Barrier for Adsorption/Desorption. To try and understand the origin of the free energy barrier, we calculated the charge density in the direction normal to the surface as a function of the distance away from the surface, which is defined as[69]

$$\rho_q(z) = \sum_i q_i \rho_i(z) \tag{13}$$

where ρ_i is the density of atom i, and q_i, its charge. The electric field can be obtained from the charge density as follows:

(69) Sokhan, V. P.; Tildesley, D. J. *Mol. Phys.* **1997**, *92*, 625.
(70) Odutola, J. A.; Dyke, T. R. *J. Chem. Phys.* **1980**, *72*, 5062.
(71) Curtiss, L. A.; Frurip, D. J.; Blander, M. *J. Chem. Phys.* **1979**, *71*.
(72) Sorenson, J. M.; Hura, G.; Glaeser, R. M.; Head-Gordon, T. *J. Chem. Phys.* **2000**, *113*, 9149.

Table 4. Transmission Coefficients, Transition Rate Constants, and Rate Constants of Adsorption and Desorption of the Three Metal Ions on the Surface

metal ion	kappa	$k_{ads.}^{TST}$ (s^{-1})	$k_{ads.}$ (s^{-1})	τ (ns)	$k_{des.}^{TST}$ (s^{-1})	$k_{des.}$ (s^{-1})	τ (ns)
magnesium	0.006 ± 0.020	3.4×10^{10}	2.0×10^{8}	5	3.8×10^{8}	2.3×10^{6}	436
calcium	0.024 ± 0.011	1.4×10^{10}	3.3×10^{8}	3	7.9×10^{9}	1.9×10^{8}	5
strontium	0.029 ± 0.021	3.0×10^{9}	8.6×10^{7}	12	1.9×10^{9}	5.5×10^{7}	18

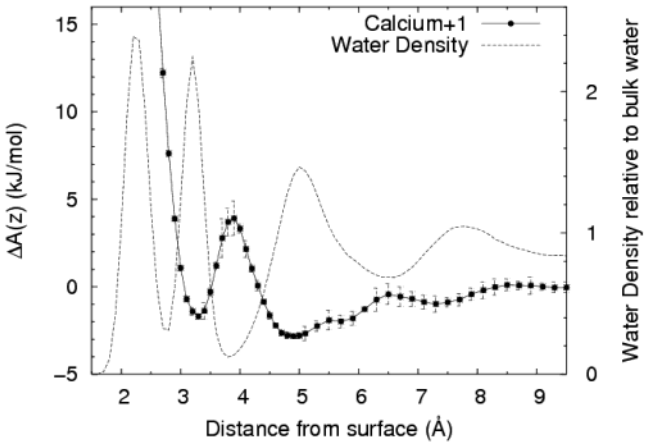

Figure 8. Fictional "calcium + 1" free energy profile as a function of distance from the surface.

$$E(z) = \frac{1}{-\epsilon_0}\int_{z_0}^{z}\rho_q(z')\,dz' \tag{14}$$

where ϵ_0 is the permittivity of vacuum. The electrostatic potential can be calculated according to

$$\Delta\varphi(z) = \varphi(z) - \varphi(z_0) = -\int_{z_0}^{z}E(z')\,dz' \tag{15}$$

The charge density and electrostatic potential as a function of distance from the surface are shown in Figure 7. The ordering of the water molecules in the vicinity of the surface causes the charge density profile to show well-defined peaks. The inner- and outer-sphere free energy minima coincide with a layer with a large excess of oxygen atoms, and the free energy barrier between them corresponds to a layer with an excess of hydrogen atoms. Hence the presence of a free energy barrier for cation adsorption corresponding to the layer with a large excess of hydrogen atoms implies that the rate of surface adsorption is mainly controlled by electrostatic forces and is much less dependent on the size of the adsorbing ion.

This hypothesis was tested by performing a new series of calculations where the charge of the calcium ion is reduced to one and all other parameters are kept constant. The new free energy profile is shown in Figure 8. The height of the free energy barrier is 6.7 kJ/mol, which is almost exactly half that of the divalent calcium ion, which supports our claim that the size of the free energy barrier is closely related to the ion charge. Moreover, the transition state position is once more at 4.0 Å away from the surface, suggesting that the transition state position is independent of the metal charge. The effect of reducing the charge to one does modify the ion by increasing its effective size with a first peak in the calcium−oxygen RDF at 2.75 Å and decreasing the water residence time in the first hydration layer to 5.6 ± 0.2 ps. However the average coordination number remains the same, i.e., 8.2. Figure 8 shows that the fictional calcium + 1 ion adsorbs as an innersphere complex at a height of 3.3 Å above the surface. At this height, it is bonded, on average, to 1.0 surface oxygen and 6.3 water oxygens with an average bond distance of 2.83 Å. The strength of the cation−water bond is now very weak, and thus almost a whole water molecule is missing from the coordination shell, the average cation−water oxygen distance is increased, and the outersphere complex is energetically preferred over the innersphere complex by about 1 kJ/mol.

C. Adsorption/Desorption Rate Calculations. Finally, we can use the method described previously in this paper, whereby we calculate the transition state rate constant of the different metal ions from their free energy profiles together with their transmission coefficient, to obtain an estimate of their rate of adsorption and desorption on the surface. We assume the reaction coordinate to be the distance between the metal ion and the surface. To calculate the transmission coefficient, we generated a pool of 750 configurations where the metal ion is constrained to be at the height above the surface corresponding to the maximum in the free energy. Then, each configuration is run for 1.4 ps, forward and backward in time, which allows us to plot the reactive flux and determine the transmission coefficient as discussed above. The transmission coefficients, transition state rate constants, rate constants, and corresponding residence times are shown in Table 4. The transmission coefficients are very low, about 1 order of magnitude smaller than those calculated for the dissociation of water from the ions' first hydration shell. This implies that comparatively high velocities are required for the cations that reach the transition state to be able to force their way through the layered and slow diffusing water structure. As noted with the cations in solution, magnesium has a much lower transmission coefficient than calcium and strontium. The uncertainties on the transmission coefficients are estimated at the 95% confidence interval of the mean when the trajectories are separated into 12 independent blocks. The size of these uncertainties is similar to that obtained for the water escaping the cations' first hydration shell but is large when compared to the value of kappa calculated here. This suggests that these results have to be taken with caution; however, they do provide us with an estimate of the order of magnitude of kappa. Table 4 shows that the three ions have similar rates of adsorption on the surface of about 10^8 s^{-1}, which corresponds to one adsorption event every few nanoseconds. The rates of desorption from the surface are similar to the adsorption rates for calcium and strontium; however, magnesium is predicted to stay adsorbed on the surface for much longer, i.e., about half a microsecond.

Conclusion

In conclusion, potential model parameters developed to model the interactions of carbonate surfaces with water were used to calculate a range of properties of metal ion−water clusters in the gas phase and in solution. We found that the calculations agreed well with experimental studies and electronic structure calculations, hence validating the transferability of our potential

model. Also, we showed that transition state theory and the analysis of the direct simulation yield the same residence times for water in the first hydration shell of calcium and strontium.

A molecular dynamics simulation of water in contact with the {10$\bar{1}$4} surface shows that the free energy of adsorption from the liquid phase is small compared to the enthalpy of adsorption calculated previously using different computational methods. This implies a large entropic change associated with the adsorption of water on the surface. To demonstrate this, we showed that the water diffusion is greatly reduced near the surface and that the surface structure imposes specific water orientation.

In the last section of this paper, we calculated the free energy profile of three metal ions adsorbing on the surface and found that there is a correlation between the relative free energy and the solvent density. The main free energy barrier associated with the formation of an innersphere complex at the mineral surface is due to electrostatic interactions of the adsorbing cation with a water layer containing a large excess of hydrogen atoms. In addition magnesium is shown to remain adsorbed on the surface for a long period of time compared to calcium and strontium. Indeed, magnesium is able to form a more stable innersphere complex due to its strong interaction with the solvent and the surface. We found a correlation between the strength of the cation−water bond and the depth of the innersphere free energy well relative to that of the outersphere complex. Cations that form a strong bond with water will be able to disrupt the water layering imposed by the presence of the surface and thus retain a full coordination shell once adsorbed on the surface.

In the future, we wish to study the adsorption of both cations and anions to stepped and defective surfaces where the growth and dissolution are thought to occur.

Acknowledgment. The authors thank Dr. A. Marmier and Dr. D. J. Cooke for useful discussions and EPSRC Grant No. GR/H0185, JREI award JR99BAPAEQ for financial support.

Supporting Information Available: Figures of the water density and average intermolecular energy, ions reactive flux, interlayer oxygen−oxygen RDF, and table of potential parameters. This material is available free of charge via the Internet at http://pubs.acs.org.

JA0487776